



Identification of the change of soluble microbial products on membrane fouling in membrane bioreactor (MBR)

Meng Yao ^a, Bradley Ladewig ^b, Kaisong Zhang ^{a,*}

^a Key Laboratory of Urban Environment and Health, Institute of Urban Environment, Chinese Academy of Sciences, Xiamen 361021, China

^b Department of Chemical Engineering, Monash University, VIC 3800, Australia

ARTICLE INFO

Article history:

Received 16 December 2010
Received in revised form 28 March 2011
Accepted 4 May 2011
Available online 14 June 2011

Keywords:

Membrane fouling
Soluble microbial products
The ratio of protein to polysaccharide
Membrane bioreactors
Fluorescence excitation emission matrix

ABSTRACT

Comprehensive fouling propensity associated with the change of soluble microbial products (SMP), especially the concentration of SMP and the ratio of protein to polysaccharide (PN/PS) has been investigated in a lab-scale submerged microfiltration MBR. Results showed that the higher ratio of PN/PS induced less irreversible fouling and improved the interaction of protein and polysaccharide to form cake layer. The rejection efficiency of major components in SMP also increased with higher PN/PS ratios. Fouling mechanisms altered from combination of intermediate pore blocking and cake formation at initial stage to cake formation on the membrane surface during long-term operation. Moreover, the irreversible fouling resistance was found to be proportional to the concentration of SMP. Lower concentration of SMP and higher PN/PS ratio should be an effective strategy in releasing membrane fouling.

© 2011 Elsevier B.V. All rights reserved.

1. Introduction

Membrane bioreactors (MBR) have been widely employed for municipal wastewater treatment. However, membrane fouling is still a major obstacle that hinders faster commercialization of MBR [1,2]. For complex liquid in MBR, which is mainly derived from each sludge fraction, namely suspended solids, colloids and dissolved substances, rapid and unexpected changes in fouling can occur. The relative contribution of individual fractions to the total fouling resistance varied substantially between studies [3–6]. For MBR treating municipal wastewater, the organic fractions in the supernatant mostly consist of SMP, which could be considered as the pool of organic compounds from substrate metabolism biomass growth and decay [7–9].

Recently, the fraction most often mentioned in relation with fouling may be the SMP. The occurrence and properties of SMP were affected by various factors such as biomass, the influent characteristics, operational conditions, sludge retention time (SRT), temperature, oxygen sources and microbial activity [10–12]. Recently reviewed by Drews, the effect of SMP on membrane fouling is still contradictory might be due to the multiple, complex and interacting influences which cannot be assessed independently of each other in lab or full-scale operation [12]. Compared with the various findings of the concentration of SMP on membrane fouling, few publications focused on the composition of SMP, especially the protein to polysaccharide

(PN/PS) ratio. The increase of specific UV absorbance and PN/PS ratio implied that the accumulated compounds in MBR supernatant were protein [13]. However, accumulation of polysaccharides rather than protein was found to decrease with increasing SRT [14]. The limited findings are still under debate.

Here, we hypothesized that the composition of SMP, especially PN/PS ratio might do important effect on membrane fouling. In our previous study, bovine serum albumin (BSA) and sodium alginate were used to evaluate membrane fouling as modeling protein and polysaccharide. The ratios of PN/PS, which regarded as the main components of SMP played an important role on membrane fouling in microfiltration (MF) [15]. However that experimental condition is far from the industrial interest of MBR.

The objective of the present research was to give a systematic investigation into fouling potential with the change of SMP, especially the ratios of PN/PS, in a lab-scale MBR. The fluorescence excitation emission matrixes (EEMs) were used to characterize the composition of SMP. The fouling propensity of different supernatant fractions was evaluated and compared by means of batch filtration experiments in a stirred cell. Furthermore, the classic fouling model for constant pressure cake filtration was applied in order to better understand the fouling process associated with the change of SMP.

2. Materials and methods

2.1. Pilot set-up

The experimental set-up used in this study is shown in Fig. 1. The MBR reactor has a working volume of 400 L. The MBR zone was

* Corresponding author. Tel.: +86 592 6190782; fax: +86 592 6190977.
E-mail address: kszhang@iue.ac.cn (K. Zhang).

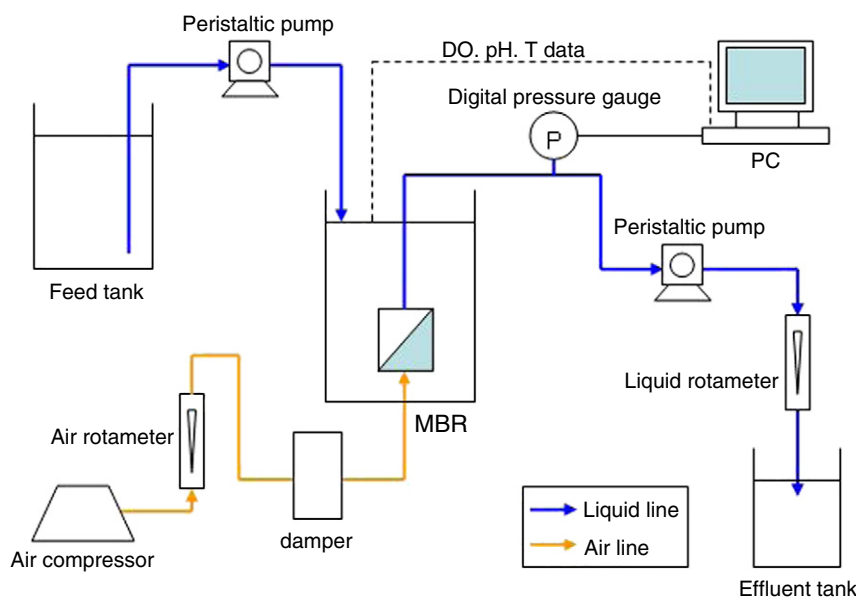


Fig. 1. MBR configuration.

installed with three 0.1 μm polyvinylidene fluoride (PVDF) flat-sheet membrane modules (SINAP-25, SINAP Membrane S&T Co., Shanghai, China). The effective filtration area of each module was 0.25 m^2 . Bubbles were injected from the bottom of the membrane module to induce a cross-flow velocity along membrane surfaces for membrane fouling control. The MBR were operated at a constant flux of 24 L/h m^2 , and the trans-membrane pressure (TMP) was monitored with a pressure gauge. Chemical cleaning-in-place procedure (0.5% (v/v) NaClO solution, 2 h duration) would be carried out if the TMP reached about 30 kPa during the operation. The synthetic wastewater used in this study mainly consisted of 750 mg/L glucose as carbon source, other components including NH_4Cl , 324 mg/L; KH_2PO_4 , 98 mg/L; peptone, 90 mg/L; yeast extract, 30 mg/L; MgSO_4 , 6.8 mg/L; FeCl_3 , 0.5 mg/L; CaCl_2 , 7.5 mg/L. The concentration of total organic carbon (TOC) was fixed at 128.5 mg/L. TOC concentration of effluent was kept as 2.55 ± 0.18 mg/L throughout the MBR operation.

2.2. Batch filtration experiments

The mixed liquor of activated sludge was collected from MBR system three times (in SRT 7th, 14th and 27th day) and filtered with a 0.45 μm -pore-size filter. The supernatant fouling potential filtration experiments were conducted in a 25 mm stirred cell with a volume of 10 ml (Model 8010, Amicon Corp.) and active surface area of 4.1 cm^2 . The membranes employed for filtration were PVDF membrane with a nominal pore size of 0.1 μm (Millipore Corp., USA). The filtration cell connected to an air-pressurized solution reservoir with a volume of 500 ml. The stirred cell and reservoir were initially filled with deionizer water (DIW) at a constant pressure (extra-dry grade nitrogen, 30 kPa) until a quasi-steady flux was attained (30 min). Then the stirred cell was refilled with the supernatant and repressurized. All filtration experiments were kept at a constant trans-membrane pressure (TMP) of 30 kPa and a stirring rate of 500 rpm (IKA RCT basic, Germany) at 22–25 $^\circ\text{C}$. After the filtration test, the membrane was rinsed by DIW for 10 s and then followed by backwash (simulated by reverse filtration) with DIW for 5 min at 30 kPa. The DIW flux recovery was measured at 30 kPa after the backwash stage. The permeate flux data was continuously collected using an electronic balance (Sartorius BS224S, Germany). With consideration of long term MBR operation, 3 cycles stirred cell tests

were conducted for each supernatant sample using the same membrane sample.

2.3. Analysis methods

The mixed liquor of activated sludge was collected from MBR system and filtered with a 0.45 μm -pore-size filter. The concentrations of protein and polysaccharide were measured by colorimetrically using the Bicinchoninic Micro Acid protein assay [16] (BioTeke Corp. China) and Anthrone method [17], respectively. BSA and glucose were used as the protein and polysaccharide standards. Humic substances were measured following modified Lowry (BioTeke Corp. China) [18]. The organic matters in the MBR supernatant and permeate were quantified by a Shimadzu analyzer (TOC-VCPH, Shimadzu, Japan). All the samples were collected at least triple and showed as an averaged value for discussion.

2.4. Fluorescence analysis

EEMs were proved to be a rapid, selective and accurate technique for capturing detailed and subtle fluorescence features that related to dissolved organic matter including SMP in water treatment [10,19]. EEMs (HITACHI F-4600 Fluorescence Spectrophotometer, Japan) were employed to obtain the EEM spectra of supernatant in MBR. Excitation (Ex) wavelength was set from 200 to 500 nm at 5 nm increments, and emission (Em) wavelength from 280 to 500 nm at 5 nm. The slits were maintained at 5 nm for both Ex and Em, and the scanning speed was set at 2400 nm/min. The photomultiplier tube (PMT) voltage was maintained at 700 V. All samples were filtered through 0.45 μm filter membrane to remove the insoluble organic particles and kept at room temperature (25 $^\circ\text{C}$) to minimize temperature influence.

The fluorescence regional integration (FRI) technique was introduced for analyzing fluorescence EEMs [20]. The EEMs were divided into five regions by horizontal and vertical lines. In general, the lower Ex (<250 nm) Em (<330 nm) mainly reflects protein type substances, such as tyrosine and aromatic protein (Regions I and II), which are low molecular weight substances. Peaks at intermediate Ex (250–340 nm) and shorter Em (<380 nm) are related to soluble microbial by-product-like material (Region III). Higher Em region (>380 nm) with lower Ex (<250 nm) region reflects fulvic acid-like substances (Region

Table 1
Amounts of supernatant components and the filtration of the membrane.

		SRT 7th	SRT 14th	SRT 27th
MLSS	mg/L ^a	2020	5590	4010
SRT	Day	7	14	27
TOC	mg/L ^a	7.55	13.27	14.55
PN/PS		0.73	2.4	0.23
Protein	Initial dissolved protein (mg/L) ^a	5.08	27.87	2.36
	Adsorbed protein ($\mu\text{g}/\text{cm}^2$) ^b	21.3 ± 7.8	54.0 ± 13.2	32.6 ± 14.7
	Rejection efficiency (%)	9.3 ± 3.4	19.3 ± 4.7	13.1 ± 5.9
Polysaccharides	Initial dissolved polysaccharides (mg/L) ^a	6.97	11.68	10.18
	Adsorbed polysaccharides ($\mu\text{g}/\text{cm}^2$) ^b	1.0 ± 0.5	7.9 ± 0.5	1.4 ± 0.9
	rejection efficiency (%)	12.0 ± 6.0	55.1 ± 3.7	11.0 ± 7.1
Humic Acid	Initial dissolved humic acid (mg/L) ^a	69.06	77.18	41.38
	Adsorbed humic acid ($\mu\text{g}/\text{cm}^2$) ^b	17.5 ± 6.4	44.2 ± 10.9	26.7 ± 12.0
	Rejection efficiency (%)	7.5 ± 2.7	16.1 ± 4.0	10.8 ± 4.8

^a These results are the average of triplet samples.

^b These results are the average of duplicated samples each with six runs (each run represents a filtration of 5 ml supernatant sample) for each filtration.

IV). Longer Ex (>250 nm) and Em (>380 nm) wavelength are related to humic acid-like organics (Region V).

The volume (ϕ_i) beneath region 'i' of the EEM can be expressed as:

$$\phi_i = \sum_{EX} \sum_{EM} I(\lambda_{ex}, \lambda_{em}) \Delta\lambda_{ex} \Delta\lambda_{em} \quad (1)$$

In which $\Delta\lambda_{ex}$ is the Ex wavelength interval (taken as 5 nm), $\Delta\lambda_{em}$ is the Em wavelength interval (taken as 5 nm), and $I(\lambda_{ex}, \lambda_{em})$ is the fluorescence intensity at each Ex/Em wavelength pair.

2.5. Resistances analysis

2.5.1. Resistances-in-series model

For the constant pressure filtration, the driving force is kept constant. According to Darcy's law, the filtration can be represented as:

$$R_t = \frac{\Delta P}{\mu J} \quad (2)$$

where J ($\text{L}/\text{h m}^2$) is the permeate flux, ΔP (Pa) is the pressure drop across the filter medium and μ (Pa·s) is the viscosity.

In order to explain permeate flux decline caused by various filtration resistance including concentration polarization, the resistance-in-series model Eq. (3) is usually used [21,22].

$$R_t = R_m + R_f + R_c \quad (3)$$

where R_t is the total or overall resistance of the system (m^{-1}). The total resistance can be split into R_m (m^{-1}), the intrinsic membrane resistance, R_f (m^{-1}), the sum of the resistances caused by pollutants adsorption in the pores or walls, R_c (m^{-1}), the resistance caused by

concentration polarization and the effect of R_c on overall resistance R_t can be removed by replacing the feed solution with DIW. R_c and R_f values will get increase with time.

2.5.2. Fouling mechanism

The fouling mechanism relevant to constant pressure dead-end filtration can be analyzed according to Hermia [23]. This method was

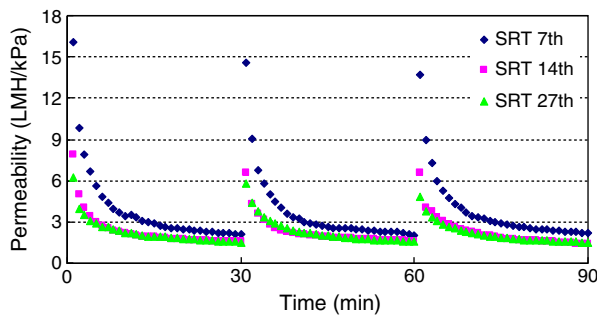


Fig. 2. Temporal changes of membrane permeability.

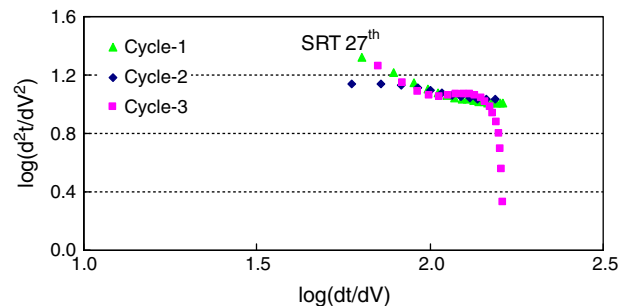
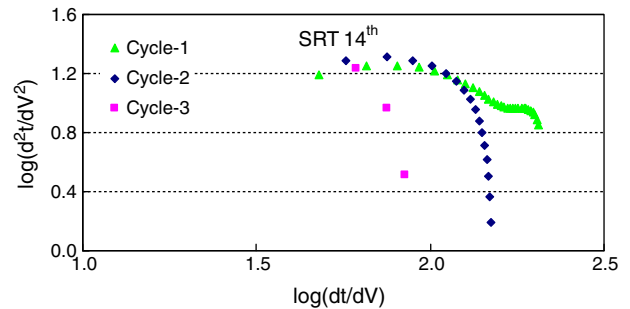
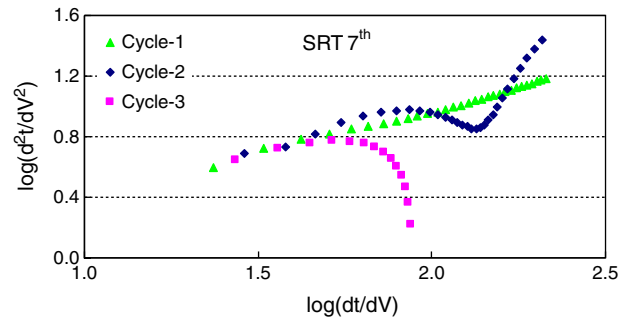


Fig. 3. Characteristic curves reflecting the fouling mechanisms during mixed liquor filtration with different SRT.

also used to identify and quantify the major organic foulants in ultrafiltration by Zheng et al. [24].

$$\frac{d^2t}{dV^2} = k \left(\frac{dt}{dV} \right)^n \quad (4)$$

Where t is filtration time, V is the total permeate volume, k is rate constant depending on n which is the flow behavior index. The four mechanisms incorporated into the model are complete pore blocking ($n = 2$), internal pore blocking ($n = 1.5$), partial pore blocking ($n = 1$), and cake formation ($n = 0$). This mechanism can be classified as internal, external, or intermediate depending on whether the fouling occurs within the pores or on the membrane. For complete blocking, it is supposed that the active membrane area is blocked by particles which are larger than the pore size. For internal pore blocking, particles smaller than pore size enter the pores and get either adsorbed or deposited in the pore. The decrease in pore volume is proportional to permeate volume on the basis of particle depositing on the pore walls. For partial pore blocking, particles might bridge a pore or block it incompletely. The effect of active membrane area reduction is similar to pore blocking but not severe. For cake filtration, it is assumed that each particle is stacked onto early arrivals at the membrane surface so as to form a cake layer.

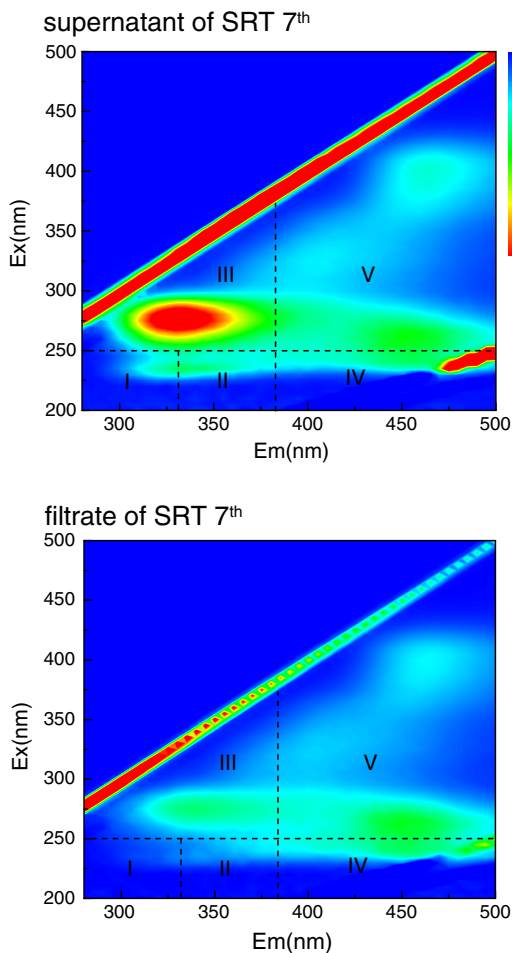


Fig. 4. EEMs characterization of the supernatant and filtrate.

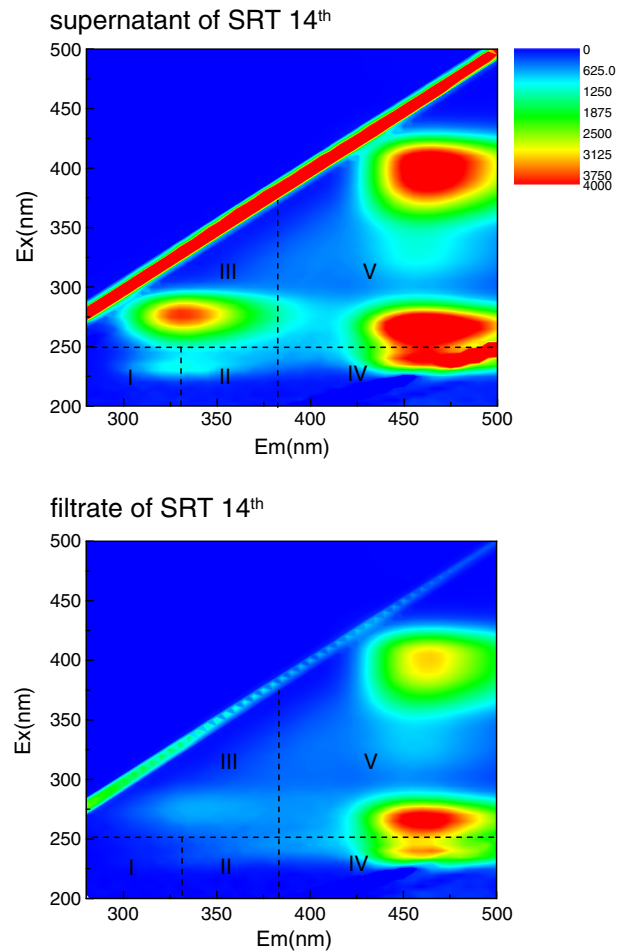


Fig. 4 (continued).

3. Results and discussion

3.1. The effect of SMP concentration change on filtration performance

The main components of the supernatant and filtrate solution were analyzed and shown in Table 1. TOC in three different stages were measured as 7.55, 13.27 and 14.55 mg/L for SRT 7th, 14th and 27th, respectively.

The changes of permeability filtrated by the supernatants in different stages are shown in Fig. 2. The supernatant with low value of TOC (sample SRT 7th) had a higher permeate flux than that with high value of TOC (sample SRT 14th). In each cycle of supernatant filtration, the permeability decline can be divided into two phases: an initial phase characterized by a rapid decline of permeability followed by a relative steady-state phase with slow decline of permeability. The fouled membrane achieved a high permeability after the cleaning procedure which was credited to the fact that much of the foulant on the membrane surface had been removed by backwashing. The recovery efficiency of membrane decreased with continuous operation.

The permeate volume versus time was analyzed to generate plots of $\log(d^2t/dV^2)$ versus $\log(dt/dV)$ according to Hermia [23]. Considering the derivation of the curve, t - V curve was conducted to fit polynomials of degree of six in each filtration process. The first cycle of filtration could be similar to the initial stage of membrane fouling in MBR. The variation of n shown in Fig. 3 indicated that the higher concentration of TOC induces worse membrane fouling at

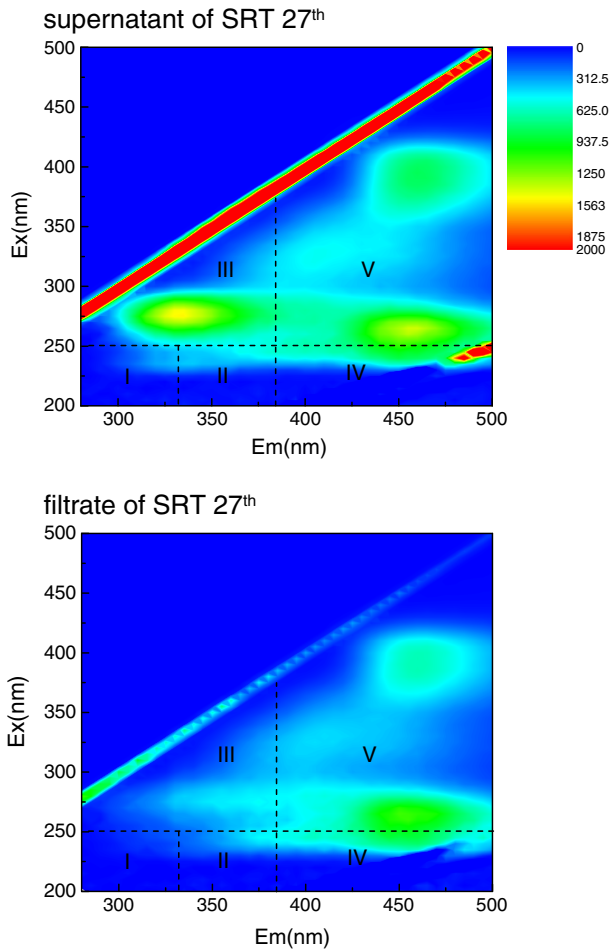


Fig. 4 (continued).

initial stage. The value of n starts from 0.59 for the supernatant TOC of 7.55 mg/L, compared with 0.43 and 0 for the supernatant TOC of 13.27 mg/L and 14.55 mg/L. All the values of n related to the filtrations ranged from 1 to 0. This might indicate that the complete blocking mode was not applicable to the case of supernatant filtration, pore plugging by comparably sized foulants was not obviously observed. With consideration of complex MBR conditions, different mechanisms might take place simultaneously and the value of n might present the combination of different mechanisms. The main fouling mechanism was generally assumed as a combination of intermediate pore blocking and cake formation. After 3 cycles, all the values of n ended as zero, which meant cake formation should be the main fouling mechanism. Linked to long term operation of MBR, alleviating the

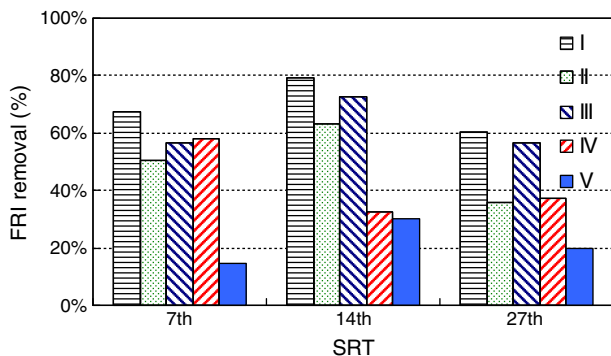


Fig. 5. FRI removal during the dead-end filtration.

cake formation should be the main strategy for fouling control. Lower concentration of SMP should be an effective way in releasing membrane fouling.

3.2. The effects of PN/PS ratio change on membrane fouling

The PN/PS ratio of the supernatant with SRT of 7 days, 14 days and 27 days was 0.73, 2.4 and 0.23, respectively. The result indicated that rejection efficiency was increasing with the PN/PS ratio (Table 1). To obtain further insight into supernatant components rejection and filtration characterization, EEMs were analyzed both for the feed solution and for the filtrate (Fig. 4). Three main fluorescence peaks were identified in the supernatant and filtrate for the three periods. Peak A was located at the Ex/Em of 275/330–335 nm, which has been described as tryptophan protein-like substances peak. The humic-like peak was observed at Ex/Em = 395–400/460–465 nm (Peak B) and fulvic acid-like peak was located around Ex/Em = 260–265/450–460 nm (Peak C). The supernatant filtration exhibited a significant rejection of protein-like substances, for the intensity reduced more than 70% of Peak A; whereas the intensity of humic and fulvic-like peaks showed reversed trend.

As shown in Fig. 5, the FRI removal rate of regions (I, II and III) related to the microbial activity was in accordance with the φ_i value. For microbial activity related regions (I, II, and III), the FRI deterioration was found to be related with PN/PS ratio (Fig. 6). The R^2 was 0.9757, 0.8937 and 0.9534 for I, II and III region respectively. The result indicated that the ratios of PN/PS are proportional to the rejection rate of microbial activity materials. It seems that protein would be like to constitute the major structure network of the gel layer. FRI removal efficiencies of fulvic-like and humic-like material were relatively lower, 32.7–57.9% and 14.6–30.0% respectively, implying that humic-like fluorescence could not be removed during MF process (Fig. 5).

With deeper investigation on filtration performance and the composition of the SMP, the ratio of PN/PS was found to have an important effect on membrane fouling. The concentrations of TOC and polysaccharide were not much different for supernatant of SRT 14th and 27th (Table 1). However, the ratio of PN/PS was 2.4 in the supernatant of SRT 14th, and nearly 10 times than that of SRT 27th (0.23) due to the different content of protein. In the tested 3 cycles, R_c induced by supernatant SRT 14th, was not much different to that induced by supernatant SRT 27th. However, R_f of supernatant SRT 27th was twice than that of supernatant SRT 14th (Table 2). Protein was supposed to interact with polysaccharides and both make joint contribution to form cake on the membrane surface.

As shown in Table 1, most of the polysaccharides (around 89%) could pass through the membrane for filtration of supernatant SRT 27th which contained less of protein, compared to only 45% of polysaccharides penetrated membrane for supernatant SRT 14th filtration. The more polysaccharides pass through the membrane pores, the more polysaccharides attach on the surface of internal pore.

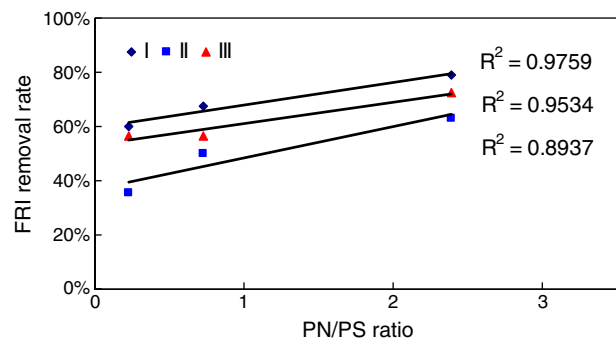


Fig. 6. The relationship between PN/PS ratio and FRI removal rate.

Table 2
Fouling resistance of microfiltration of supernatant.

		R_m ($\times 10^{11} \text{ m}^{-1}$)	R_t	R_c ($\times 10^{12} \text{ m}^{-1}$)	R_c/R_t (%)	R_f ($\times 10^{11} \text{ m}^{-1}$)	R_f/R_t (%)	R_t ($\times 10^{12} \text{ m}^{-1}$)
SRT 7th	Cycle-1	1.76	8.63	1.84	90.20	0.26	1.27	2.04
	Cycle-2	1.76	8.22	1.92	89.72	0.41	1.92	2.14
	Cycle-3	1.76	8.89	1.74	87.88	0.61	3.08	1.98
SRT 14th	Cycle-1	1.76	6.26	2.45	87.19	1.84	6.55	2.81
	Cycle-2	1.76	6.52	2.23	82.60	2.98	11.04	2.70
	Cycle-3	1.76	5.71	2.49	80.84	4.10	13.31	3.08
SRT 27th	Cycle-1	2.02	7.01	2.31	80.21	3.69	12.81	2.88
	Cycle-2	2.02	7.35	1.95	70.91	5.98	21.75	2.75
	Cycle-3	2.02	6.80	1.90	63.97	8.65	29.12	2.97

This might be the reason of the higher R_f of supernatant SRT 27th than that of supernatant SRT 14th.

The rejected polysaccharides would accumulate and interact with protein to form cake layer on membrane surface, the continuous shear resulted in aggregate components interaction which could promote the consolidation of biopolymer. The ratio of PN/PS played an important role on the interaction between protein and polysaccharide, and also on the relative membrane fouling. In this experiment, the ratio of PN/PS in supernatant SRT 14th seems to be more effective to promote proteins and polysaccharides interaction, and then induce cake formation.

4. Conclusions

In this study, comprehensive investigations of fouling propensity of SMP during MF filtration of MBR were carried out in a stirred cell. The following conclusions have been drawn.

The dominant fouling mechanism for supernatant MF filtration was assumed to cake formation. The irreversible fouling resistance was found to be proportional to the TOC concentration of supernatant. The PN/PS ratio was confirmed to have a significant effect on membrane fouling. The ratios of PN/PS were proportional to the rejection rate of microbial activity materials especially protein and polysaccharides. The higher ratio induced less irreversible fouling and improved the interaction of protein and polysaccharide to form cake layer within the three tested conditions.

Acknowledgment

The authors gratefully acknowledge the support by the Knowledge Innovation Project of Chinese Academy of Science (Project no. KZCX2-YW-452) and the National Nature Science Foundation of China (Grant no. 50708090). The authors also thank Hongyuan Luo for the help of sample analysis.

References

- [1] P. Le-Clech, V. Chen, A.G. Fane, Fouling in membrane bioreactors used in wastewater treatment, *J. Membr. Sci.* 284 (2006) 17–53.
- [2] F. Meng, S.R. Chae, A. Drews, H.S. Shin, F. Yang, Recent advances in membrane bioreactors (MBRs): membrane fouling and membrane material, *Water Res.* 43 (2009) 1489–1512.
- [3] J. Wu, X. Huang, Effect of mixed liquor properties on fouling propensity in membrane bioreactors, *J. Membr. Sci.* 342 (2009) 88–96.
- [4] S. Rosenberger, C. Laabs, B. Lesjean, R. Gnirss, G. Amy, M. Jekel, J.C. Schrotter, Impact of colloidal and soluble organic material on membrane performance in membrane bioreactors for municipal wastewater treatment, *Water Res.* 40 (2006) 710–720.
- [5] X.M. Wang, T.D. Waite, Role of gelling soluble and colloidal microbial products in membrane fouling, *Environ. Sci. Technol.* 43 (2009) 9341–9347.
- [6] K.K. Ng, S.K. Lateef, S.C. Panchangam, P.A. Hong, P.Y. Yang, The effect of soluble microbial products on membrane fouling in a fixed carrier biological system, *Sep. Purif. Technol.* 72 (2010) 98–104.
- [7] A. Drews, J. Mante, V. Iversen, M. Vocks, B. Lesjean, M. Kraume, Impact of ambient conditions on SMP elimination and rejection in MBRs, *Water Res.* 41 (2007) 3850–3858.
- [8] C. Jarusutthirak, G. Amy, Role of soluble microbial products (SMP) in membrane fouling and flux decline, *Environ. Sci. Technol.* 40 (2006) 969–974.
- [9] D.J. Barker, D.C. Stuckey, A review of soluble microbial products (SMP) in wastewater treatment systems, *Water Res.* 33 (1999) 3063–3082.
- [10] Z.P. Wang, T. Zhang, Characterization of soluble microbial products (SMP) under stressful conditions, *Water Res.* 44 (2010) 5499–5509.
- [11] H.S. Shin, S.T. Kang, Characteristics and fates of soluble microbial products in ceramic membrane bioreactor at various sludge retention times, *Water Res.* 37 (2003) 121–127.
- [12] A. Drews, Membrane fouling in membrane bioreactors—characterisation, contradictions, cause and cures, *J. Membr. Sci.* 363 (2010) 1–28.
- [13] B.X. Thanh, C. Visvanathan, M. Spérandio, R.B. Aim, Fouling characterization in aerobic granulation coupled baffled membrane separation unit, *J. Membr. Sci.* 318 (2008) 334–339.
- [14] H.Y. Ng, T.W. Tan, S.L. Ong, Membrane fouling of submerged membrane bioreactors: impact of mean cell residence time and the contributing factors, *Environ. Sci. Technol.* 40 (2006) 2706–2713.
- [15] M. Yao, K. Zhang, L. Cui, Characterization of protein-polysaccharide ratios on membrane fouling, *Desalination* 259 (2010) 11–16.
- [16] B.J. Olsen, J. Markwell, Assays for the determination of protein concentration, *Curr. Protoc. Protein Sci.* (2007) 14–17.
- [17] Thomas G. Ludwig, Hyman J.V. Goldberg, The anthrone method for the determination of carbohydrates in foods and in oral rinsing, *J. Dent. Res.* 35 (1956) 90–94.
- [18] B. Frølund, T. Griebe, P.H. Nielsen, Enzymatic activity in the activated sludge floc matrix, *Appl. Microbiol. Biotechnol.* 43 (1995) 755–761.
- [19] Z. Wang, Z. Wu, S. Tang, Characterization of dissolved organic matter in a submerged membrane bioreactor by using three-dimensional excitation and emission matrix fluorescence spectroscopy, *Water Res.* 43 (2009) 1533–1540.
- [20] W. Chen, P. Westerhoff, J.A. Leenheer, K. Booksh, Fluorescence excitation–emission matrix regional integration to quantify spectra for dissolved organic matter, *Environ. Sci. Technol.* 37 (2003) 5701–5710.
- [21] C. Fersi, L. Gzara, M. Dhahbi, Flux decline study for textile wastewater treatment by membrane processes, *Desalination* 244 (2009) 321–332.
- [22] N. Maximous, G. Nakhla, W. Wan, Comparative Assessment of hydrophobic and hydrophilic membrane fouling in wastewater applications, *J. Membr. Sci.* 339 (2009) 93–99.
- [23] J. Hermia, Constant pressure blocking filtration laws—application to power-law non-Newtonian fluids, *Trans. Inst. Chem. Eng.* 60 (1982) 183–187.
- [24] X. Zheng, M. Ernst, M. Jekel, Identification and quantification of major organic foulants in treated domestic wastewater affecting filterability in dead-end ultrafiltration, *Water Res.* 43 (2009) 238–244.